Time-Averaged Pressure of Fluctuating Gas Motion in Small-Diameter Tubes

Zbyszko Kazimierski* and Janusz Trojnarski†
Technical University of Lodz, Lodz, Poland

The problem relates mainly to the unsteady pressure measuring systems when they contain any type of pneumatic transmission line. Such a line usually has the form of a tube or bore of small diameter. A variation of the time-averaged pressure along the tube appears when the relative pressure amplitude at the tube inlet is significant. This is caused by summation of nonlinear effects of the gas motion inside the tube. The viscous and heat conducting gas is considered. The aim of the present work is to determine the relation between time-averaged pressure at the inlet and at the end of the tubes. The unsteady, compressible boundary-layer equations for axisymmetrical gas flow in the tube were adopted as the basic equations of the problem. The perturbation method has been used for solution of the equations. A first-order linear solution is presented in literature. A new second-order solution has been derived herein. The results of calculations for single tubes and for systems of two consecutive tubes of different diameters are presented in a form convenient for practical use. The qualitative and quantitative agreement of the theoretical results with available experimental data has been found.

Nomenclature

a_0 = mean sound velocity at the tube inlet, m/s
C_p, C_v = specific heats, J/kg · K
i = imaginary unit, $=\sqrt{-1}$
K = wave transfer number, $=p_0R^2/\mu a_0 L$
L = tube length, m, see Fig. 1
Pr = Prandtl number, $=\mu C_p/\lambda$
p = dimensionless pressure, related to p_0
p_0 = mean pressure at the tube inlet, N/m^2
R = internal tube radius, m, see Fig. 1
s = shear wave number used in first-order solution, $=(\kappa\omega K)^{\frac{1}{2}}$, Ref. 2
T = dimensionless temperature, related to T_0
T_0 = mean temperature at the tube inlet, K
t = time, s
u, v = dimensionless components of velocity, related to a_0
V_k = measuring volume, m^3, see Fig. 1
ϵ = relative pressure amplitude at the tube inlet, related to p_0
η = dimensionless radial coordinate, related to R
κ = isentropic expansion index, $=C_p/C_v$
λ = gas heat conductivity, W/m · s
μ = viscosity, kq/ms
ξ = dimensionless axial coordinate, related to L
s = dimensionless density, related to s_0
s_0 = mean density at the tube inlet, kg/m^3
τ = dimensionless time $=\Omega t$
ϕ = phase lag, rad, $=\text{arctg}(-p_{1s}/p_{1c})$, see Fig. 2
Ω = frequency, rad/s
ω = dimensionless frequency, $\Omega L/a_0$

Subscripts

1 = first-order perturbations, first tube
2 = second-order perturbations, second tube
10 = time-averaged values of right-hand sides of Eqs. (11–14)
20 = time-averaged values of second-order perturbations
c = real part
s = imaginary part
z = complex amplitude

Introduction

THE pressure measuring technique in an unsteady gas stream faces serious problems when the pressure signal is transmitted pneumatically from the port of a pitot tube or a wall hole to the point where it is sensed. The transmission line usually has the form of a tube or bore of small diameter compared to its length. In many devices, this line is arranged in form of consecutive tubes of different diameters, with or without a large measuring volume attached to the end of the last tube. In some arrangements, the last tube is followed by a low-frequency, high-sensitivity pressure transducer, in others, by a common liquid-column manometer.

It is well known that the steady pressure occurring at the end of the transmission line does not represent the true time-averaged value of the pressure at the probe port. This is due to summation of nonlinear effects of the pulsating gas motion inside the small-diameter long tube.

One current method of measuring the time-dependent pressure is to use special high-frequency miniature pressure transducers. The fluctuating pressure is directly sensed by the transducer located in the measurement point. In many practical applications, however, it is necessary to connect the measurement point (e.g., on an airfoil surface) with the transducer face by means of a comparatively long bore of small diameter. The relation between the time-dependent pressure at the bore inlet and at the transducer face depends on the characteristics of the pressure wave propagation through this bore. It appears that the determination of the time-averaged pressure is an essential problem to be solved for pressure measuring systems with pneumatic transmission lines, apart from the kind of the pressure transducers applied.

Received Nov. 11, 1985; revision received June 2, 1986.

*Professor of Fluid Mechanics.
†Research Scientist.

Although the problem of time-average fluctuating gas pressure measurement with traditional pressure probes has been known for more than 50 years, the number of relevant published works is not very large. Fundamental experimental information on the problem can be found in Refs. 3–6. The results presented in these papers show that the time-averaged pressure error is still one of the most important problems of the flow measurement technique. A purely experimental approach, however, seems to be in serious doubt because of the large number of parameters introduced and the complexity of the problem. So the experiments have to be supported by a theoretical treatment, which is difficult because of the need to deal with time-dependent differential equations for compressible, viscous, and heat-conducting gas.

The approach presented in Refs. 9 and 10 employing a typical one-dimensional, nonlinear gas flow model supplemented with a set of simplified, unsteady boundary-layer equations cannot be considered a useful one. This model is devoted to relatively "wide" tubes where the question of energy dissipation is of limited interest.

The most accurate theoretical descriptions of the problem originate from a set of unsteady, compressible boundary-layer equations, for axially symmetrical gas flow in small-diameter tubes. This model is employed in Refs. 1–3 and 8. The perturbation method is usually used to solve the equations. The effectiveness of the perturbation method for this aim is clearly argued by Telionis.[7]

Theoretical results obtained for the case of a strong temperature gradient along the tube given in Ref. 8, but no references to the time-averaged pressure change are presented. The time-averaged pressure variation has been calculated in Ref. 3 where the set of the unsteady boundary-layer equations are simplified by introducing three unknown functions determined at the tube wall: pressure, viscous shear stress, and heat flux density. Although the assumptions made during this transformation arouse some doubts, they are fully acceptable for strongly damping tubes for which the wave transfer number $K \approx 1$.

Bergh and Tijdeman[1,2] solve the problem in the linear formulation (first-order terms in the perturbation method), when the time-averaged pressure is assumed constant along the tube axis. The linear formation can be considered a good approximation if the relative amplitude of the pulsating pressure at the tube inlet is very small. When this relative amplitude is significant, a variation of the time-averaged pressure along the tube axis due to nonlinear effects has to be taken into account.

The aim of the present work is to determine the relation between time-averaged pressure at the inlet and at the end of the small-diameter tubes shown schematically in Fig. 1. A new second-order solution of the problem has been derived in this paper. The first-order, linear solution presented in Refs. 1 and 2 is exploited for effective calculation of these second-order results. The experimental results received by Klonowicz[3] are used for verification of the time-averaged pressure obtained here theoretically. Preliminary comparisons with the experimental results presented in Ref. 4 are also very promising.

Theoretical Calculations

The following assumptions connected with the gas flow and tube geometry were used:

1) The internal radius of the tube or bore R is very small as compared with its length L.

2) The gas is viscous and heat conducting.

3) The gas motion is unsteady, laminar, and axisymmetrical.

4) The gas parameters μ, λ, C_p, and C_v are constant.

5) The nondimensional gas pressure at the tube inlet is given by the formula,

$$p(0,\tau) = 1 + \epsilon e^{i\tau}$$

6) The tube wall is isothermal, with the gas temperature at the wall T_0 equal to a constant wall temperature.

7) The gas temperature in the measuring volume V_k (see Fig. 1) is constant and equal to T_0.

8) The time-averaged mass flow rate through the tube is equal to zero.

If the assumption $R/L \ll 1$ is introduced into the complete set of differential equations governing the unsteady, axially symmetric flow of viscous and heat-conducting ideal gas, the result can be called the boundary-layer approach for tubes of small diameter.

Introducing nondimensional notation according to the definitions given in the Nomenclature, the nondimensional form of these equations is as follows.

Equations of motion:

$$\kappa s\left(\omega\frac{\partial u}{\partial \tau} + u\frac{\partial u}{\partial \xi} + \frac{L}{R}v\frac{\partial u}{\partial \eta}\right) = -\frac{\partial p}{\partial \xi} + \frac{1}{K}\left(\frac{\partial^2 u}{\partial \eta^2} + \frac{1}{\eta}\frac{\partial u}{\partial \eta}\right) \tag{1}$$

$$\frac{\partial p}{\partial \eta} = 0, \quad \text{i.e.,} \quad p = p(\xi,\tau) \tag{2}$$

Equation of continuity:

$$\omega\frac{\partial s}{\partial \tau} + u\frac{\partial s}{\partial \xi} + \frac{L}{R}v\frac{\partial s}{\partial \eta} + s\frac{\partial u}{\partial \xi} + s\frac{L}{R}\left(\frac{\partial v}{\partial \eta} + \frac{v}{\eta}\right) = 0 \tag{3}$$

Equation of state:

$$p = sT \tag{4}$$

Equation of energy:

$$\kappa s\left(\omega\frac{\partial T}{\partial \tau} + u\frac{\partial T}{\partial \xi} + \frac{L}{R}v\frac{\partial T}{\partial \eta}\right) = (\kappa - 1)\left[\omega\frac{\partial p}{\partial \tau} + u\frac{\partial p}{\partial \xi} + \frac{1}{K}\left(\frac{\partial u}{\partial \eta}\right)^2\right] + \frac{1}{PrK}\left(\frac{\partial^2 T}{\partial \eta^2} + \frac{1}{\eta}\frac{\partial T}{\partial \eta}\right) \tag{5}$$

The nondimensional parameters, the wave damping number $1/K$ and the nondimensional frequency ω (which plays the role of the Strouchal number), are defined in the Nomenclature. The assumed ranges of their variations, $K \leq 40$ and $\omega \leq 4\pi$, do not violate the boundary-layer approximation. The wave length, e.g., for $\omega = 4\pi$, is still much longer than the tube radius R. Besides, at high frequencies, a new very thin oscillatory layer proportional to $R/\sqrt{\omega}$ appears.[7]

The solutions of Eqs. (1–5) are assumed in the form of the following series:

$$\begin{aligned} p(\xi,\tau) &= 1 + \epsilon p_1(\xi,\tau) + \epsilon^2 p_2(\xi,\tau) + \ldots \\ s(\xi,\eta,\tau) &= 1 + \epsilon s_1(\xi,\eta,\tau) + \epsilon^2 s_2(\xi,\eta,\tau) + \ldots \\ T(\xi,\eta,\tau) &= 1 + \epsilon T_1(\xi,\eta,\tau) + \epsilon^2 T_2(\xi,\eta,\tau) + \ldots \\ u(\xi,\eta,\tau) &= 0 + \epsilon u_1(\xi,\eta,\tau) + \epsilon^2 u_2(\xi,\eta,\tau) + \ldots \\ v(\xi,\eta,\tau) &= 0 + \epsilon v_1(\xi,\eta,\tau) + \epsilon^2 v_2(\xi,\eta,\tau) + \ldots \end{aligned} \tag{6}$$

where ϵ denotes the small parameter of this problem. According to assumption 5, ϵ is the relative pressure amplitude at the tube inlet. Some remarks on the convergence of Eqs. (6) will be presented in the last part of this paper.

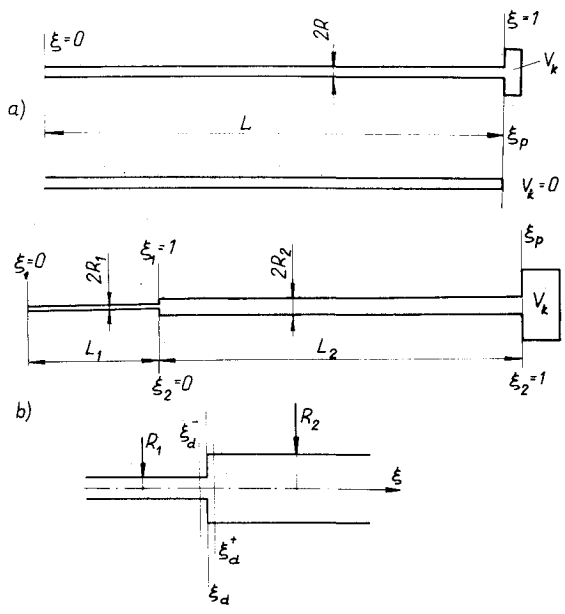

Fig. 1 Tube system schematics.

The postulated form of Eqs. (6) are introduced into the basic equations (1–5) and the resulting terms are ordered with respect to the powers of ϵ. The sequence of the following differential equations was received. Equations of first order:

$$\kappa\omega\frac{\partial u_1}{\partial\tau} = -\frac{\partial p_1}{\partial\xi} + \frac{1}{K}\frac{1}{\eta}\frac{\partial}{\partial\eta}\left(\eta\frac{\partial u_1}{\partial\eta}\right) \tag{7}$$

$$-\omega\frac{\partial s_1}{\partial\tau} = \frac{\partial u_1}{\partial\xi} + \frac{L}{R}\frac{1}{\eta}\frac{\partial}{\partial\eta}(\eta v_1) \tag{8}$$

$$s_1 = p_1 - T_1 \tag{9}$$

$$\kappa\omega\frac{\partial T_1}{\partial\tau} = \omega(\kappa-1)\frac{\partial p_1}{\partial\tau} + \frac{1}{PrK}\frac{1}{\eta}\frac{\partial}{\partial\eta}\left(\eta\frac{\partial T_1}{\partial\eta}\right) \tag{10}$$

Equations of second order:

$$\kappa\omega\frac{\partial u_2}{\partial\tau} + \frac{\partial p_2}{\partial\xi} - \frac{1}{K}\frac{1}{\eta}\frac{\partial}{\partial\eta}\left(\eta\frac{\partial u_2}{\partial\eta}\right) = -\kappa\left[\omega\frac{\partial}{\partial\tau}(s_1u_1) + \frac{\partial}{\partial\xi}(u_1u_1) + \frac{L}{R}\frac{1}{\eta}\frac{\partial}{\partial\eta}(u_1v_1\eta)\right] \tag{11}$$

$$\omega\frac{\partial s_2}{\partial\tau} + \frac{\partial u_2}{\partial\xi} + \frac{L}{R}\frac{1}{\eta}\frac{\partial}{\partial\eta}(\eta v_2) = -\left[\frac{\partial}{\partial\xi}(s_1u_1) + \frac{L}{R}\frac{1}{\eta}\frac{\partial}{\partial\eta}(\eta s_1v_1)\right] \tag{12}$$

$$p_2 - T_2 - s_2 = s_1T_1 \tag{13}$$

$$\kappa\omega\frac{\partial T_2}{\partial\tau} - \omega(\kappa-1)\frac{\partial p_2}{\partial\tau} - \frac{1}{PrK}\frac{1}{\eta}\frac{\partial}{\partial\eta}\left(\eta\frac{\partial T_2}{\partial\eta}\right) = -\kappa\left[\omega\frac{\partial}{\partial\tau}(s_1T_1) + \frac{\partial}{\partial\xi}(u_1T_1) + \frac{L}{R}\frac{1}{\eta}\frac{\partial}{\partial\eta}(\eta v_1T_1) + (\kappa-1)\left[u_1\frac{\partial p_1}{\partial\xi} + \frac{1}{K}\left(\frac{\partial u_1}{\partial\eta}\right)^2\right]\right] \tag{14}$$

The right-hand sides of Eqs. (11–14) are nonlinear but known functions, which will be fully defined after solving Eqs. (7–10).

Solution of First-Order Equations

According to assumption 5, the solutions of Eqs. (7–10) have the following form:

$$p_1(\xi,\tau) = \mathcal{R}e\left[p_{1z}(\xi)e^{i\tau}\right];\ p_{1z} = p_{1c} + ip_{1s}$$

$$s_1(\xi,\eta,\tau) = \mathcal{R}e\left[s_{1z}(\xi,\eta)e^{i\tau}\right];\ s_{1z} = s_{1c} + is_{1s} \tag{15}$$

and similarly for T_1, u_1, and v_1.

The analytical solutions for the complex amplitudes of first order p_{1z}, T_{1z}, s_{1z}, u_{1z}, and v_{1z} have been presented in Refs. 1 and 2. An excellent experimental confirmation of these results is described in Ref. 1.

The complex amplitude $p_{1z} = p_{1z}(\xi = 1, \omega, K)$ is very important in the design of unsteady pressure measuring systems. For this reason, some unpublished results of calculations of the absolute value of $|p_{1z}|$ and its phase lag ϕ will be given in the next part of this paper.

Solution of Second-Order Equations

The nonlinear right-hand sides of Eqs. (11–14) can be generally written in the form

$$F(\xi,\eta,\tau) = F_{10}(\xi,\eta) + \mathcal{R}e\left[F_{1z}(\xi,\eta)e^{2i\tau}\right] \tag{16}$$

where F_{10} denotes the nonvanishing time averaged part of $F(\xi,\eta,\tau)$. See Ref. 7.

Taking into account the above form of the right-hand sides of Eqs. (11–14) and the boundary condition at the tube inlet (see assumption 5), it can be stated that the solution of the second-order equations are as follows:

$$\begin{aligned}
p_2(\xi,\tau) &= p_{20}(\xi) + \mathcal{R}e\left[p_{2z}(\xi)e^{2i\tau}\right]\\
s_2(\xi,\eta,\tau) &= s_{20}(\xi,\eta) + \mathcal{R}e\left[s_{2z}(\xi,\eta)e^{2i\tau}\right]\\
T_2(\xi,\eta,\tau) &= T_{20}(\xi,\eta) + \mathcal{R}e\left[T_{2z}(\xi,\eta)e^{2i\tau}\right]\\
u_2(\xi,\eta,\tau) &= u_{20}(\xi,\eta) + \mathcal{R}e\left[u_{2z}(\xi,\eta)e^{2i\tau}\right]\\
v_2(\xi,\eta,\tau) &= v_{20}(\xi,\eta) + \mathcal{R}e\left[v_{2z}(\xi,\eta)e^{2i\tau}\right]
\end{aligned} \tag{17}$$

The nonvanishing time-averaged terms of these solutions are the main subject of this paper. The complex amplitudes of second-order solutions p_{2z}, s_{2z} ... will be the object of the next part of this work. The set of differential equations for the time-averaged terms of Eqs. (17) can be easily derived from the set of Eqs. (11–14). One then obtains

$$\frac{\partial p_{20}}{\partial\xi} - \frac{1}{K}\frac{1}{\eta}\frac{\partial}{\partial\eta}\left(\eta\frac{\partial u_{20}}{\partial\eta}\right) = f_{10}(\xi,\eta) \tag{18}$$

$$\frac{\partial u_{20}}{\partial\xi} + \frac{L}{R}\frac{1}{\eta}\frac{\partial}{\partial\eta}(v_{20}\eta) = g_{10}(\xi,\eta) \tag{19}$$

$$p_{20} - T_{20} - s_{20} = \overline{s_2T_1} \tag{20}$$

$$-\frac{1}{PrK}\frac{1}{\eta}\frac{\partial}{\partial\eta}\left(\eta\frac{\partial T_{20}}{\partial\eta}\right) = h_{10}(\xi,\eta) \tag{21}$$

Equation (21) for the function T_{20} is decoupled, so the solution for function p_{20} will be achieved on the basis of Eqs. (18) and (19) only.

According to Eqs. (11) and (12) the right-hand sides of Eqs. (18) and (19) are given by

$$\begin{aligned}
f_{10}(\xi,\eta) &= -\kappa\left[\frac{\partial}{\partial\xi}(\overline{u_1u_1}) + \frac{L}{R}\frac{1}{\eta}\frac{\partial}{\partial\eta}(\eta\overline{u_1v_1})\right]\\
g_{10}(\xi,\eta) &= -\left[\frac{\partial}{\partial\xi}(\overline{s_1u_1}) + \frac{L}{R}\frac{1}{\eta}\frac{\partial}{\partial\eta}(\eta\overline{s_1v_1})\right]
\end{aligned} \tag{22}$$

The time-averaged products denoted in Eqs. (22) by overbars are calculated according to the following procedure:

$$u_1 = \mathcal{R}e\left[(u_{1c} + iu_{1s})\,e^{i\tau}\right], \qquad s_1 = \mathcal{R}e\left[(s_{1c} + is_{1s})\,e^{i\tau}\right]$$

$$\overline{u_1 s_2} = \tfrac{1}{2}(u_{1c}s_{1c} + u_{1s}s_{1s}) \tag{23}$$

and similarly for $\overline{u_1 u_1}$, $\overline{u_1 v_1}$, and $\overline{s_1 v_1}$.

Taking into consideration that $\partial u_{20}/\partial\eta$ has a finite value for $\eta = 0$, one can obtain from Eq. (18)

$$u_{20}(\xi,\eta) = \frac{K\eta^2}{4}\frac{\partial p_{20}}{\partial\xi} + K\kappa\left\{\int\frac{1}{\eta}\left[\int\frac{\partial}{\partial\xi}(\overline{u_1 u_1})\,\eta\,d\eta\right]d\eta + \frac{L}{R}\int(\overline{u_1 v_1})\,d\eta\right\} + G(\xi) \tag{24}$$

Introducing the function

$$\varphi(\xi,\eta) = \int\frac{1}{\eta}\left[\int\frac{\partial}{\partial\xi}(\overline{u_1 u_1})\,\eta\,d\eta\right]d\eta + \frac{L}{R}\int(\overline{u_1 v_1})\,d\eta \tag{25}$$

and taking into account that $u_{20}(\xi,1) = 0$, $G(\xi)$ can be determined and Eq. (24) is expressed as

$$u_{20}(\xi,\eta) = \frac{K}{4}\frac{\partial p_{20}}{\partial\xi}(\eta^2 - 1) + K\kappa[\varphi(\xi,\eta) - \varphi(\xi,1)] \tag{26}$$

Multiplication of Eq. (19) by η and further integration in the limits $0 \le \eta \le 1$ yields

$$\frac{\partial}{\partial\xi}\int_0^1 u_{20}(\xi,\eta)\,\eta\,d\eta = -\frac{\partial}{\partial\xi}\int_0^1(\overline{u_1 s_1})\,\eta\,d\eta \tag{27}$$

By introducing Eq. (26) into Eq. (27) and integrating twice with respect to ξ, one obtains

$$p_{20}(\xi) = 16\int\left\{\frac{1}{K}\int_0^1(\overline{u_1 s_1})\,\eta\,d\eta + \kappa\int_0^1[\varphi(\xi,\eta) - \varphi(\xi,1)]\,\eta\,d\eta\right\}d\xi + C\xi + D \tag{28}$$

It can be easily proved that for the closed tube system, when the time-averaged value of the mass flow rate is equal to zero, the constant C in Eq. (28) is equal to zero as well.

The zero mass flow rate through the closed tube system, in the second-order approximation, is described by

$$\int_0^1(u_{20} + \overline{s_1 u_1})\,\eta\,d\eta = 0 \tag{29}$$

It should be noted that a closed measuring volume V_k attached to the end of the tube does not change Eq. (29).

By substituting u_{20} defined by Eq. (26) and $\int_0^1(\overline{s_1 u_1})\,\eta\,d\eta$ from Eq. (28) into Eq. (29), one can check that $C = 0$.

The only additive constant D in Eq. (28) can be calculated from the boundary conditions, which depend on the tube system geometry.

For the single tube shown in Fig. 1a, this boundary condition is determined at the tube inlet ($\xi = 0$). According to assumption 5: $p_{20}(0) = 0$.

For the tube with one radius discontinuity placed at $\xi = \xi_d$ (Fig. 1b), an additional condition has to be introduced,

$$p_{20}(\xi_d^-) = p_{20}(\xi_d^+)$$

The algorithm described in this section has been realized in the form of the pressure averaging in thin tubes (PATT) computer program.

Results

The general geometry of the tube system introduced into PATT program is that illustrated in Fig. 1b. It includes two consecutive tubes of different diameter, with a closed measuring volume V_k attached to the end of the second tube. The single closed-end tube is covered by the program as a simpler case of the above scheme.

A calculation of the undefined integrals of the products $\overline{u_1 u_2}$, $\overline{u_1 v_1}$, and $\overline{u_1 s_1}$ that exist in Eqs. (25) and (28) have been accomplished numerically by using the spline function approximation.

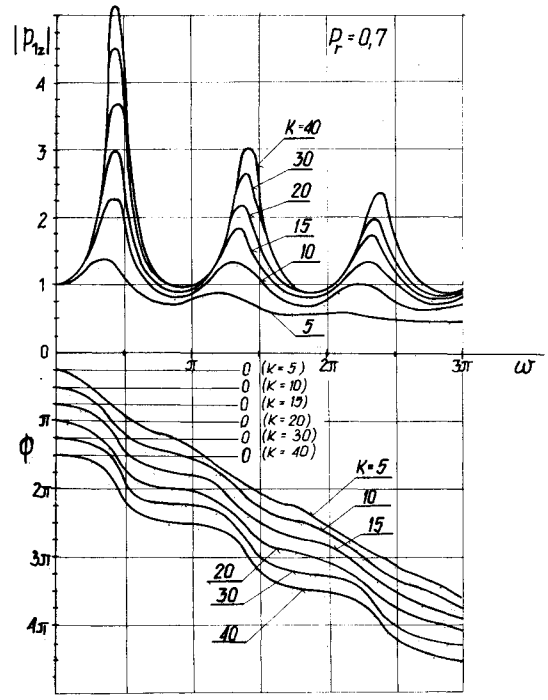

Fig. 2 Absolute value and phase lag of first-order perturbation for pressure p_{1z}.

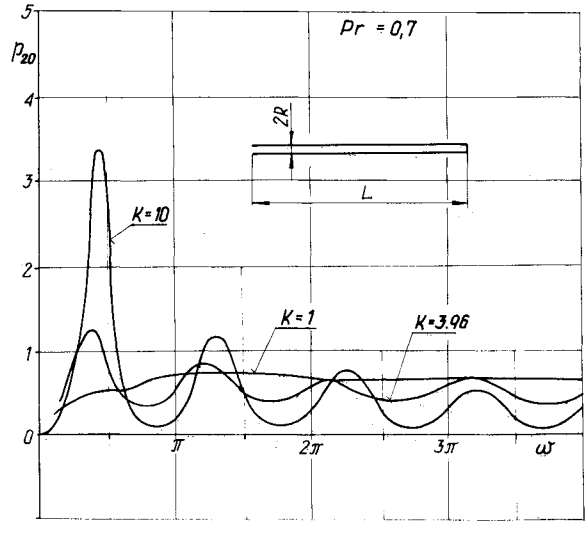

Fig. 3 Time-averaged value of second-order perturbation for pressure p_{20}.

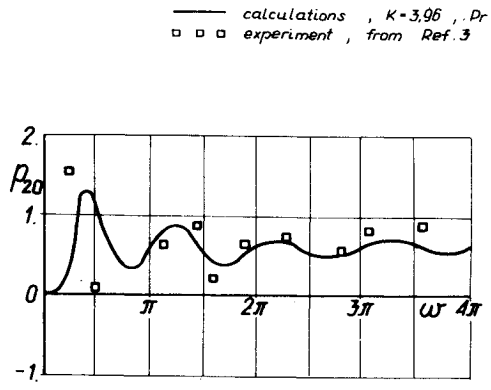

Fig. 4 Calculated and experimentally obtained p_{20}.

For the system shown in Fig. 1a with $V_k = 0$, both the absolute value and phase lag of $p_{1z} = p_{1z}(\xi = 1, \omega, K)$ are presented in Fig. 2. Such a presentation is very convenient for practical use and is not available in the literature.

The function $p_{20} = p_{20}(\xi = 1, \omega, K)$ for the single closed-end tube ($V_k = 0$), is presented in Fig. 3. The relative difference between the time-averaged pressure at the inlet and at the end of the tube (the pressure is related to p_0) is equal to $\epsilon^2 p_{20}$. For example, if $\epsilon = 0.2$ and $p_{20} = 1$, this relative difference reaches 4%.

A comparison between the present theoretical results and the experimental data of Klonowicz[3] is shown in Fig. 4. Time-averaged pressure measurement is still a very difficult task; thus, the experimental data given in Ref. 3 must be considered in light of the relatively high uncertainty range. The agreement between the theory and experiment can be estimated from Fig. 4.

Some selected results for two consecutive tubes with one discontinuity in the tube radius and $V_k = 0$ are shown in Fig.

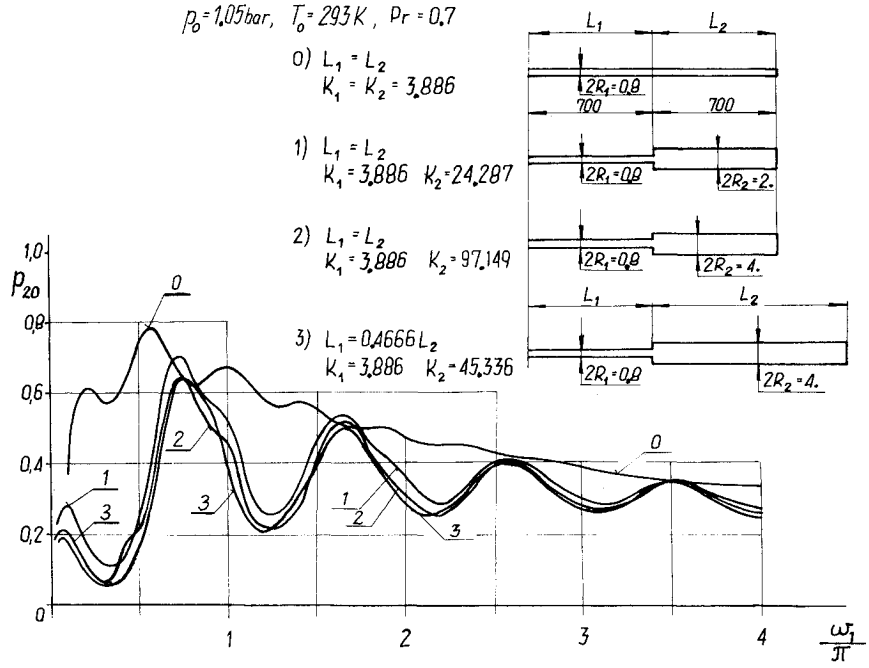

Fig. 5 Influence of second tube proportions on p_{20} in second tube (dimensions in mm).

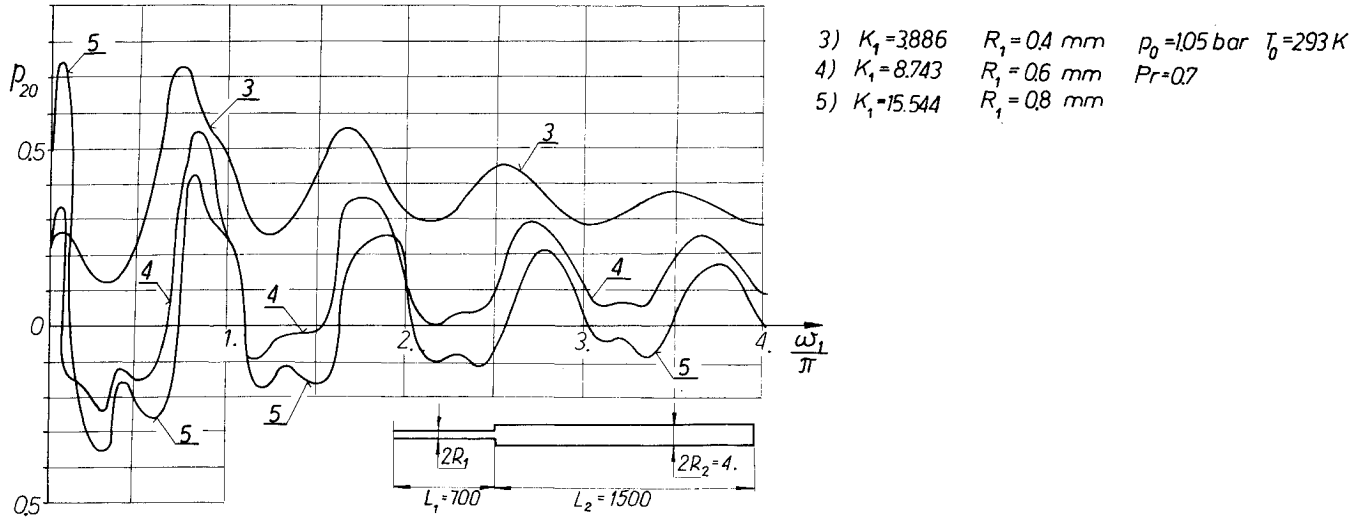

Fig. 6 Influence on first tube radius variation on p_{20} in second tube (dimensions in mm).

5. These diagrams show the influence of an increase in volume of the second tube on the time-averaged pressure at the end of that tube.

The nondimensional frequency and wave transfer numbers specified in Figs. 5 and 6 are defined as

$$\omega_1 = \frac{\Omega L_1}{a_0} \qquad K_1 = \frac{p_0 R_1^2}{\mu a_0 L_1} \qquad K_2 = \frac{p_0 R_2^2}{\mu a_0 L_2} \tag{30}$$

The influence of variations in the radius of the first tube on p_{20} in the second tube is presented in Fig. 6. Curve 3 is obtained for a very thin, strongly damping first tube and curves 4 and 5 for some first tubes with less damping.

Conclusions

The question of the convergence of Eqs. (6) is substantial in the mathematical approach used in the present work. One can state that the convergence will be ensured if the maximum values of the functions $p_1, p_2 \ldots$ and $s_1, s_2 \ldots$ are of order one for a given value of K in the whole domain of ω under consideration. The numerical analysis performed proves that this condition is fulfilled for $K \leq 40$.

The wave transfer number K plays an essential role in the analysis of the pulsating gas flow in tubes. $1/K$ determines the damping properties of the tube and thus may be called the wave damping number.

The resonant values of p_{20} (for $K > 1$), shown for a single-closed-end tube in Fig. 3, appear at frequencies close to the resonant frequencies of the first-order solutions exhibited in Fig. 2. Moreover for the single-closed-end-tube, the values of p_{20} are always positive (Fig. 3).

The nonzero measuring volume V_k does not introduce any qualitative difference in $p_{20} = p_{20}(\xi = 1, \omega, K)$ for the single tube. Quantitatively, p_{20} is usually lower for $V_k > 0$ than for $V_k = 0$.

An examination of the two consecutive tube system leads to the conclusions outlined below.

An increase of the second tube volume beyond a certain value, at the same K_1, has very small influence on $p_{20}(\xi_2 = 1, \omega, K_2)$, as was shown in Fig. 5. The experimental diagrams obtained in Ref. 4 are qualitatively similar to that shown in Fig. 6, but a quantitative comparison with the experiment reported in Ref. 4 is impossible here. This is because the pressure wave at the tube inlet, generated by Krause et al.,[4] differs significantly from the harmonic wave assumed in the present work. The arbitrary pressure wave shape at the tube inlet will be considered in the next phase of the present work.

For the tube systems described in Figs. 5 and 6 and marked by numbers 2-5, the difference between p_{20} at the end ($\xi_2 = 1$) and at the inlet ($\xi_2 = 0$) of the second tube is negligibly small.

Negative values of p_{20} may appear in the second tube for a certain ratios of the first and second tube radii, as is shown in Fig. 6. Some experimental results reported in Refs. 3-5 confirm the possibility of such a phenomenon.

The calculations performed by means of the PATT program for various arrangements of two consecutive tubes show that the relative time-averaged pressure correction $\epsilon^2 p_{20}$ at the second tube end can be minimized by a proper selection of the tube dimensions. Nevertheless, the maximum value of $\epsilon^2 p_{20}$ resulting from Figs. 5 and 6, calculated for, e.g., $\epsilon = 0.2$, reaches 3.0%. This example shows the importance of the presented analysis in the pressure measuring technique.

References

[1] Bergh, H. and Tijdeman, H., "Theoretical and Experimental Results for the Dynamic Response of Pressure Measuring Systems," Amsterdam, NLR, Rept. TR F.238, Jan. 1965.

[2] Tijdeman, H., "On the Propagation of Sound Waves in Cylindrical Tubes," *Journal of Source and Vibration*, Vol. 42, Jan. 1975, p. 1.

[3] Klonowicz, W., "Measurement of the Time Averaged Fluctuating Gas Pressure with Thin Tubes," Ph.D. Thesis, Univ. of Strathclyde, Glasgow and Technical Univ. of Lodz, Poland, 1985.

[4] Krause, L.N., Dudzinski, T.J., and Johnson, R.C., "Total Pressure Averaging in Pulsating Flows," *ISA Transactions*, Vol. 13, No. 2, 1974.

[5] Weyer, H., "Bestimmung der zeitlichen Druckmittelwerte in stark fluktuierenden Stroemung, insbesondere in Turbomaschinen," DFVLR FB 74-34, 1974.

[6] Kronauer, R.E. and Grant, H.P., "Pressure Probe Response in Fluctuating Flow," *Proceedings of 2nd U.S. National Congress of Applied Mechanics*, ASME, New York, 1954.

[7] Telionis, D.P., *Unsteady Viscous Flows*, Springer-Verlag, New York, Berlin, 1981.

[8] Rott, N., "Damped and Thermally Driven Acoustic Oscillations in Wide and Narrow Tubes," *ZAMP*, Vol. 20, 1969, p. 230.

[9] Chester, W., "Resonant Oscillations in Closed Tubes," *Journal of Fluid Mechanics*, Vol. 18, 1964, p. 44.

[10] Van Buren, A.L., "Mathematical Model for Non-Linear Standing Waves in a Tube," *Journal of Sound and Vibration*, Vol. 42, No. 3, 1975, p. 273.